

An Alternative Calculation of the Size-of-Source Effect Uncertainty for Non-uniform Sources

M. J. Martín · J. P. Pérez · V. Chimenti

Published online: 18 March 2008
© Springer Science+Business Media, LLC 2008

Abstract For a correct determination of the size-of-source effect (SSE), it is necessary to use a large (e.g., 50-mm diameter) radiation source of uniform spectral radiance. The non-uniformity of the source can be an important component of the uncertainty because it is difficult to obtain sources with good uniformity over the whole aperture. In the indirect method to measure the SSE, the component due to the source non-uniformity comes from the measurement of $S(L, \infty)$, usually measured outside the spot that blocks radiation from the radiation thermometer target. By expressing the SSE as an experimental sum of successive contributions of radiating rings at the source aperture, the uncertainty due to the non-uniformity can be reduced. In this article, the calculus of the SSE and its uncertainty for the usual equation is compared with the calculus based on an experimental equation that considers the SSE as a sum of the contributions from radiating rings.

Keywords Indirect method · Integrating sphere · Non-uniformity · Size-of-source effect · Uncertainty

1 Introduction

The signal from a radiation thermometer (RT) can be shown experimentally to depend on the target size. At different distances, an RT will have different nominal target sizes, depending on the field of view defined by the optics. Ideally, a correct measurement is performed when the nominal field of view is completely filled by the target to be measured. In practice, this is not possible due to the limitations of the optics of an RT. As a result of the inclusion of radiation originating outside the nominal target area

M. J. Martín (✉) · J. P. Pérez · V. Chimenti
Centro Español de Metrología (CEM), C/del Alfar, 2, 28760 Tres Cantos, Madrid, Spain
e-mail: mjmartin@cem.mityc.es

and the loss (e.g. scattering) of radiation originating from within it, the temperature indicated will depend on the size of the source. This phenomenon is known as the size-of-source effect, or SSE. The SSE is a consequence of radiation scattering by dust particles, reflections between lens surfaces, diffraction, and aberrations in the optical system of an RT [1].

For a correct determination of the SSE, it is necessary to use a radiation source of uniform spectral radiance with an aperture much larger than the nominal target size of the RT. Usually, two methods are used: the direct and the indirect methods [2,3]. In the indirect method, the nominal target area of the RT is filled by a black spot, which blocks the radiation from the target. The radiation originating outside the nominal target area that reaches the detector of the RT is measured.¹ The SSE for a source of radius r , $\sigma(r, r_0)$, is determined as²

$$\sigma(r, r_0) = \frac{S(L, r) - S(L, r_0)}{S(L, \infty)} \quad (1)$$

where $S(L, r)$ is the detected signal for a source of radius r , $S(L, r_0)$ is the detected signal for a source of radius r_0 , r_0 is the radius of the spot blocking the nominal target, and $S(L, \infty)$ is the signal detected for an ideal source of infinite radius. In practice, we cannot provide an infinite radius, therefore, $S(L, \infty)$ is approximated by the signal measured outside the black spot. In the indirect method, the numerator of Eq. 1 is measured directly and therefore it can be considered more accurate than the direct one.

2 Measurements

2.1 Instrumentation

The equipment used to measure the SSE by the indirect method consists of:

- a CEM-constructed integrating sphere of 450-mm diameter with a 100-mm diameter aperture
- several apertures of different radii (5, 7.5 mm, ...) made of black cardboard
- a glass plate with a black cardboard spot of 3-mm diameter pasted on it
- a Xenophot lamp (24 V, 260 W) mounted inside the sphere, with a DC power supply

The two RTs used here are:

- a IKE LP2 with a central wavelength of 650 nm and a nominal target radius of 0.42 mm at a distance of 67 cm between the source and the objective
- a VEGA TSP 2.11 with a central wavelength of 900 nm and a nominal target area 0.99 mm × 1.32 mm at a distance of 66 cm between the source and the objective

¹ The black spot should block the nominal target area of the RT. As the target area is not a well-defined variable (it depends on the manufacturer's viewpoint), it is recommended to use the smallest black spot that causes an abrupt decrease in the signal of the RT.

² Experimentally, the dark current, d , should be subtracted from the three signals in Eq. 1. In the denominator, it is assumed that $d \ll S(L, \infty)$.

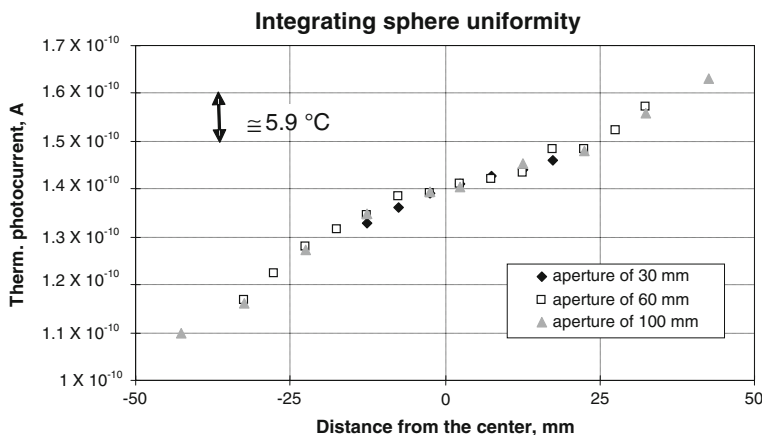


Fig. 1 Integrating sphere uniformity measured for three apertures at 650 nm

The integrating sphere uniformity was measured for three aperture diameters (30, 60, and 100 mm) and the results obtained with the LP2 are shown in Fig. 1.

2.2 Procedures

2.2.1 Classic Uncertainty Calculation Using Indirect Method

Equation 1 can be expressed as

$$\sigma(r, r_0) = \frac{\Delta S(L, r, r_0) - S_b}{S(L, \infty) - S_b} \cong \frac{\Delta S(L, r, r_0) - S_b}{S(L, \infty)} \quad (2)$$

where $\Delta S(L, r, r_0)$ is the thermometer signal measured at the center of the spot, S_b is the thermometer signal from the spot measured when $r = r_0$, and $S(L, \infty)$ is the thermometer signal measured on the source outside the spot. It is assumed that $S(L, \infty) \gg S_b$. The measurements are performed as follows:

- (1) The signal of the RT detector is measured when an aperture of the same radius as the black spot is placed in front of the source (background). Ideally, this is zero ($S(L, r_0) - S(L, r_0)$), but it may not be the case because residual radiation is transmitted by, and reflected from, the black spot. This signal is S_b and it is subtracted from the rest of the measurements with different apertures. However, as we are using a black spot to block the radiation from the target, S_b is likely to vary with aperture size when the aperture of the sphere is open, there is more radiation in the room (radiation exits the sphere and some of it will find its way onto the black spot, probably by reflecting off the lens of the thermometer). This extra background radiation will be different for different aperture sizes. For a correct measurement, the black spot should have as low a reflectance as possible—ideally the black spot should be a miniature blackbody or an equivalent radiation trap.

- (2) An aperture of radius $r_i > r_0$ is placed in front of the source and two signals are measured: one with the RT focused on the black spot, $\Delta S(r_i, r_0)$, and another focused on the ring formed between the black spot and the aperture, $S_i(L, \infty)$. Therefore, for each aperture i , we determine

$$\sigma(r_i, r_0) = \frac{\Delta S(r_i, r_0) - S_b}{S_i(L, \infty)} \quad (3)$$

To estimate the non-uniformity of the source, two values of $S_i(L, \infty)$ are measured: one at the center of the right side, $S_i^{\text{right}}(L, \infty)$, of the radiation ring and another one at the left side, $S_i^{\text{left}}(L, \infty)$, and we take $S_i(L, \infty)$ as the average.

The combined standard uncertainty of $\sigma(r_i, r_0)$ can be obtained using the law of propagation of uncertainties applied to Eq. 3;^{3,4}

$$\begin{aligned} u^2(\sigma(r_i, r_0)) &= \left(\frac{\partial \sigma(r_i, r_0)}{\partial S_i(L, \infty)} \right)^2 u^2(S_i(L, \infty)) + \left(\frac{\partial \sigma(r_i, r_0)}{\partial \Delta S(r_i, r_0)} \right)^2 u^2(\Delta S(r_i, r_0)) \\ &\quad + \left(\frac{\partial \sigma(r_i, r_0)}{\partial S_b} \right)^2 u^2(S_b) \\ &= s_{1i}^2 u^2(S_i(L, \infty)) + s_{2i}^2 u^2(\Delta S(r_i, r_0)) + s_{3i}^2 u^2(S_b) \end{aligned} \quad (4)$$

The sensitivity coefficients can be calculated as

$$s_{1i} = -\frac{\Delta S(r_i, r_0) - S_b}{S_i^2(L, \infty)} = -\frac{\sigma(r_i, r_0)}{S_i(L, \infty)} \quad (5)$$

$$s_{2i} = \frac{1}{S_i(L, \infty)} \quad (6)$$

$$s_{3i} = -\frac{1}{S_i(L, \infty)} \quad (7)$$

2.2.2 Uncertainty Calculation Using Successive Radiating Rings

A different method to calculate the SSE experimentally is given here, with a more realistic combined standard uncertainty, maintaining the formal method of estimation. To minimize the effect of non-uniformity, the SSE is expressed as the sum of contributions from consecutive rings.

³ We have considered that r_i, r_0 are fixed quantities. A more complete uncertainty analysis taking into account the uncertainties in r_i and r_0 , should follow [4] based on an empirical model for the shape of the SSE curve.

⁴ We measure all ΔS and S with the same thermometer, so we should consider the correlation. Nevertheless, we estimate the contribution to the uncertainty as the repeatability of the measurements (see Sect. 2.2.3), and in this case, they are independent measurements.

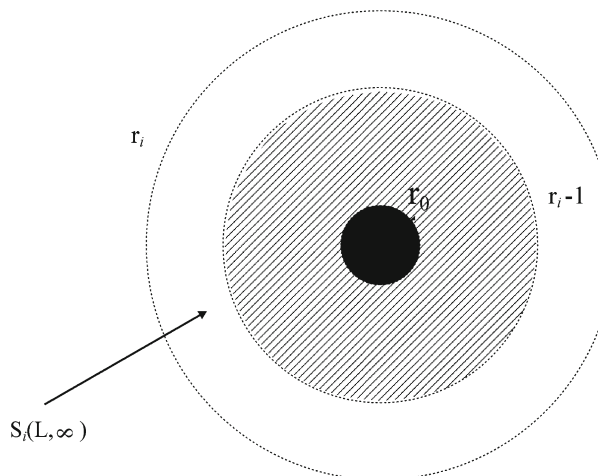


Fig. 2 $S_i(L, \infty)$ measurements of SSE

The experimental procedure is similar to the one described in the previous section except for step 2. When $r_i > r_1$, the values of $S_i^{\text{right}}(L, \infty)$ and $S_i^{\text{left}}(L, \infty)$ are measured at the center of the right and the left sides of the radiating ring between r_i and r_{i-1} (see Fig. 2).⁵ For the first aperture, the SSE is

$$\sigma(r_1, r_0) = \frac{\Delta S(r_1, r_0) - S_b}{S_1(L, \infty)} \quad (8)$$

For the second aperture, SSE can be expressed as

$$\sigma(r_2, r_0) = \frac{\Delta S(r_2, r_0) - \Delta S(r_1, r_0)}{S_2(L, \infty)} + \sigma(r_1, r_0) \quad (9)$$

For an aperture i , Eq. 9 can be generalized;

$$\sigma(r_i, r_0) = \frac{\Delta S(r_1, r_0) - S_b}{S_1(L, \infty)} + \sum_{j=2}^i \frac{\Delta S(r_j, r_0) - \Delta S(r_{j-1}, r_0)}{S_j(L, \infty)} \quad (10)$$

In this way, the contribution of each ring is based on the value of its radiation and the uncertainty due to the non-uniformity of the source is associated only with the contribution of each ring to the total SSE.

⁵ Notice that the radiation from $r < r_i$ is not blocked, only the radiation thermometer target is placed at the area $r_{i-1} < r < r_i$.

The expression of the combined standard uncertainty for each ring is obtained from Eq. 10 using the law of propagation of uncertainties:

$$\begin{aligned}
 u^2(\sigma(r_i, r_0)) &= \sum_{j=1}^i \left(\frac{\partial \sigma(r_i, r_0)}{\partial S_j(L, \infty)} \right)^2 u^2(S_j(L, \infty)) \\
 &\quad + \sum_{j=1}^i \left(\frac{\partial \sigma(r_i, r_0)}{\partial \Delta S(r_j, r_0)} \right)^2 u^2(\Delta S(r_j, r_0)) + \left(\frac{\partial \sigma(r_i, r_0)}{\partial S_b} \right)^2 u^2(S_b) \\
 &= \sum_{j=1}^i s'_{1ij}^2 u^2(S_j(L, \infty)) + \sum_{j=1}^i s'_{2ij}^2 u^2(\Delta S(r_j, r_0)) + s'_{3i}^2 u^2(S_b) \quad (11)
 \end{aligned}$$

The sensitivity coefficients s'_{1ij} , s'_{2ij} , and s'_{3i} are:

$$s'_{1ij} = \begin{cases} s'_{1i1} = -\frac{\Delta S(r_1, r_0) - S_b}{S_1^2(L, \infty)} \\ s'_{1ij} = -\frac{\Delta S(r_j, r_0) - \Delta S(r_{j-1}, r_0)}{S_j^2(L, \infty)} \end{cases} \quad \text{for } j = 2, \dots, i \quad (12)$$

$$s'_{2ij} = \begin{cases} \frac{1}{S_j(L, \infty)} - \frac{1}{S_{j+1}(L, \infty)} & \text{for } j = 1 \text{ to } i \\ \frac{1}{S_i(L, \infty)} & \text{for } j = i \end{cases} \quad (13)$$

$$s'_{3i} = -\frac{1}{S_1(L, \infty)} \quad (14)$$

2.2.3 Uncertainties

The uncertainties are estimated as:

- $u(\Delta S(r, r_0))$: standard uncertainty due to the repeatability of the measurements on the spot, calculated as the mean standard deviation of 10 measurements taken with each aperture.
- $u(S_b)$: standard uncertainty due to the repeatability of the measurements of the background, calculated as the mean standard deviation of 10 measurements taken when the aperture is equal to the spot.
- $u(S(L, \infty))$: standard uncertainty due to the source non-uniformity, estimated as the difference between the value on the right side and the value on the left side, for each aperture, assuming a rectangular probability distribution.

3 Results

Table 1 shows the results obtained for the classic method for the IKE LP2 thermometer and Table 2 for the VEGA thermometer. Tables 3 and 4 show the calculus of the uncertainty. Looking at Tables 3 and 4, it appears that $U(\sigma)$ increases strongly with aperture

Table 1 SSE results for IKE LP2 radiation thermometer (650 nm)

| Aperture radius r_i (mm) | Therm. signal at the spot $\Delta S(r_i, r_0)$ (V) | Therm. signal at the right side of the ring, $S_i^{\text{right}}(L, \infty)$ (V) | t_{right} (°C) | Therm. signal at the left side of the ring, $S_i^{\text{left}}(L, \infty)$ (V) | t_{left} (°C) | Therm. signal out of the spot, $S_i(L, \infty)$ (V) | σ |
|-------------------------------|---|---|-------------------------|---|------------------------|--|----------|
| 1.5 | -3.208×10^{-5} | – | – | – | – | – | 0.0000 |
| 5.0 | -1.270×10^{-5} | 6.353×10^{-2} | 1061.3 | 6.106×10^{-2} | 1058.1 | 6.229×10^{-2} | 0.0003 |
| 7.5 | 6.337×10^{-6} | 6.395×10^{-2} | 1061.8 | 6.071×10^{-2} | 1057.6 | 6.233×10^{-2} | 0.0006 |
| 10.0 | 1.817×10^{-5} | 6.471×10^{-2} | 1062.8 | 6.055×10^{-2} | 1057.4 | 6.263×10^{-2} | 0.0008 |
| 12.5 | 3.525×10^{-5} | 6.540×10^{-2} | 1063.6 | 5.997×10^{-2} | 1056.6 | 6.268×10^{-2} | 0.0011 |
| 15.0 | 4.566×10^{-5} | 6.547×10^{-2} | 1063.7 | 5.961×10^{-2} | 1056.2 | 6.254×10^{-2} | 0.0012 |
| 17.5 | 5.021×10^{-5} | 6.563×10^{-2} | 1063.9 | 5.898×10^{-2} | 1055.3 | 6.230×10^{-2} | 0.0013 |
| 20.0 | 5.675×10^{-5} | 6.662×10^{-2} | 1065.1 | 5.871×10^{-2} | 1054.9 | 6.266×10^{-2} | 0.0014 |
| 25.0 | 6.868×10^{-5} | 6.841×10^{-2} | 1067.3 | 5.835×10^{-2} | 1054.4 | 6.338×10^{-2} | 0.0016 |
| 30.0 | 8.140×10^{-5} | 6.965×10^{-2} | 1068.7 | 5.865×10^{-2} | 1054.9 | 6.415×10^{-2} | 0.0018 |
| 35.0 | 1.047×10^{-4} | 7.006×10^{-2} | 1069.2 | 5.855×10^{-2} | 1054.7 | 6.430×10^{-2} | 0.0021 |
| 50.0 | 1.162×10^{-4} | 7.214×10^{-2} | 1071.6 | 5.315×10^{-2} | 1047.0 | 6.264×10^{-2} | 0.0024 |

Table 2 SSE results for VEGA radiation thermometer (900 nm)

| Aperture radius r_i (mm) | Therm. signal at the spot $\Delta S(r_i, r_0)$ (V) | Therm. signal at the right side of the ring, $S_i^{\text{right}}(L, \infty)$ (V) | t_{right} (°C) | Therm. signal at the left side of the ring, $S_i^{\text{left}}(L, \infty)$ (V) | t_{left} (°C) | Therm. signal out of the spot, $S_i(L, \infty)$ (V) | σ |
|-------------------------------|---|---|-------------------------|---|------------------------|--|----------|
| 1.5 | -2.456×10^{-5} | – | – | – | – | – | 0.0000 |
| 5.0 | 6.523×10^{-4} | 1.434×10^{-1} | 811.4 | 1.375×10^{-1} | 808.3 | 1.404×10^{-1} | 0.0048 |
| 7.5 | 8.486×10^{-4} | 1.439×10^{-1} | 811.6 | 1.378×10^{-1} | 808.4 | 1.408×10^{-1} | 0.0062 |
| 10.0 | 9.660×10^{-4} | 1.451×10^{-1} | 812.2 | 1.369×10^{-1} | 808.0 | 1.410×10^{-1} | 0.0070 |
| 12.5 | 1.058×10^{-3} | 1.473×10^{-1} | 813.3 | 1.372×10^{-1} | 808.1 | 1.422×10^{-1} | 0.0076 |
| 15.0 | 1.103×10^{-3} | 1.484×10^{-1} | 813.9 | 1.367×10^{-1} | 807.8 | 1.425×10^{-1} | 0.0079 |
| 17.5 | 1.151×10^{-3} | 1.478×10^{-1} | 813.6 | 1.362×10^{-1} | 807.6 | 1.420×10^{-1} | 0.0083 |
| 20.0 | 1.174×10^{-3} | 1.494×10^{-1} | 814.4 | 1.361×10^{-1} | 807.5 | 1.427×10^{-1} | 0.0084 |
| 25.0 | 1.301×10^{-3} | 1.509×10^{-1} | 815.1 | 1.360×10^{-1} | 807.5 | 1.434×10^{-1} | 0.0092 |
| 30.0 | 1.368×10^{-3} | 1.528×10^{-1} | 816.1 | 1.384×10^{-1} | 808.8 | 1.456×10^{-1} | 0.0096 |
| 35.0 | 1.473×10^{-3} | 1.545×10^{-1} | 816.9 | 1.367×10^{-1} | 807.8 | 1.456×10^{-1} | 0.0103 |
| 50.0 | 1.775×10^{-3} | 1.643×10^{-1} | 821.5 | 1.286×10^{-1} | 803.4 | 1.464×10^{-1} | 0.0123 |

radius, due to the $u(S(L, \infty))$ uncertainty component. This component is estimated in a very conservative way, based on the large influence of the source non-uniformity (see differences between $S_i^{\text{right}}(L, \infty)$ and $S_i^{\text{left}}(L, \infty)$ in Tables 1 and 2).

Table 5 shows the results obtained with the successive rings method for the IKE LP2 thermometer and Table 6 for the VEGA thermometer. Tables 7 and 8 show the calculus of the uncertainty.

The results above are shown graphically in Fig. 3 (squares correspond to the classic method and circles to the method using successive radiation rings).

The uncertainty calculus of the SSE measurements depends strongly on the non-uniformity of the source used. Sometimes, this non-uniformity can be an important

Table 3 SSE uncertainty results for IKE LP2 radiation thermometer (650 nm)

| Aperture radius r_i (mm) | σ | $s_{2i}^2 u^2(\Delta S(r_i, r_0))$ | $s_{3i}^2 u^2(S_b)$ | $s_{1i}^2 u^2(S(L, \infty))$ | $U(\sigma) k = 2$ |
|----------------------------|----------|------------------------------------|------------------------|------------------------------|-------------------|
| 1.5 | 0.0000 | — | — | — | — |
| 5.0 | 0.0003 | 1.34×10^{-10} | 1.39×10^{-10} | 1.27×10^{-11} | 0.00003 |
| 7.5 | 0.0006 | 2.46×10^{-10} | 1.39×10^{-10} | 8.55×10^{-11} | 0.00004 |
| 10.0 | 0.0008 | 2.66×10^{-10} | 1.37×10^{-10} | 2.37×10^{-10} | 0.00005 |
| 12.5 | 0.0011 | 1.88×10^{-10} | 1.37×10^{-10} | 7.21×10^{-10} | 0.00006 |
| 15.0 | 0.0012 | 8.56×10^{-11} | 1.38×10^{-10} | 1.13×10^{-9} | 0.00007 |
| 17.5 | 0.0013 | 1.07×10^{-10} | 1.39×10^{-10} | 1.66×10^{-9} | 0.00009 |
| 20.0 | 0.0014 | 1.43×10^{-10} | 1.37×10^{-10} | 2.67×10^{-9} | 0.00011 |
| 25.0 | 0.0016 | 1.69×10^{-10} | 1.34×10^{-10} | 5.31×10^{-9} | 0.00015 |
| 30.0 | 0.0018 | 6.00×10^{-11} | 1.31×10^{-10} | 7.67×10^{-9} | 0.00018 |
| 35.0 | 0.0021 | 8.03×10^{-11} | 1.30×10^{-10} | 1.21×10^{-8} | 0.00022 |
| 50.0 | 0.0024 | 1.78×10^{-10} | 1.37×10^{-10} | 4.29×10^{-8} | 0.00042 |

Table 4 SSE uncertainty results for VEGA radiation thermometer (900 nm)

| Aperture radius r_i (mm) | σ | $s_{2i}^2 u^2(\Delta S(r_i, r_0))$ | $s_{3i}^2 u^2(S_b)$ | $s_{1i}^2 u^2(S(L, \infty))$ | $U(\sigma) k = 2$ |
|----------------------------|----------|------------------------------------|------------------------|------------------------------|-------------------|
| 1.5 | 0.0000 | — | — | — | — |
| 5.0 | 0.0048 | 3.45×10^{-12} | 2.13×10^{-12} | 3.42×10^{-9} | 0.00012 |
| 7.5 | 0.0062 | 2.18×10^{-10} | 2.12×10^{-12} | 6.01×10^{-9} | 0.00016 |
| 10.0 | 0.0070 | 5.62×10^{-10} | 2.11×10^{-12} | 1.39×10^{-8} | 0.00024 |
| 12.5 | 0.0076 | 3.04×10^{-11} | 2.08×10^{-12} | 2.43×10^{-8} | 0.00031 |
| 15.0 | 0.0079 | 8.48×10^{-12} | 2.07×10^{-12} | 3.51×10^{-8} | 0.00037 |
| 17.5 | 0.0083 | 5.45×10^{-12} | 2.08×10^{-12} | 3.81×10^{-8} | 0.00039 |
| 20.0 | 0.0084 | 2.27×10^{-11} | 2.06×10^{-12} | 5.10×10^{-8} | 0.00045 |
| 25.0 | 0.0092 | 1.49×10^{-11} | 2.04×10^{-12} | 7.68×10^{-8} | 0.00055 |
| 30.0 | 0.0096 | 1.31×10^{-11} | 1.98×10^{-12} | 7.46×10^{-8} | 0.00055 |
| 35.0 | 0.0103 | 1.21×10^{-11} | 1.98×10^{-12} | 1.32×10^{-7} | 0.00073 |
| 50.0 | 0.0123 | 1.14×10^{-11} | 1.96×10^{-12} | 7.48×10^{-7} | 0.00173 |

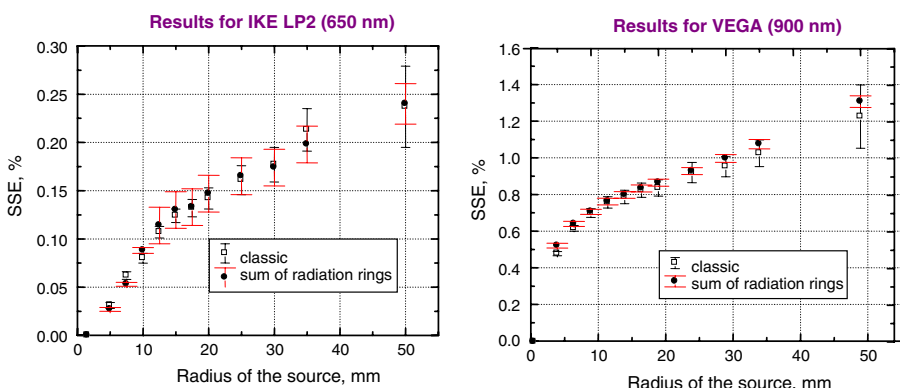
**Fig. 3** Results obtained for (a) IKE LP2 and (b) VEGA; squares for results obtained using Eq. 3 and circles for Eq. 10

Table 5 SSE results for IKE LP2 radiation thermometer using successive radiation rings (650 nm)

| Aperture radius r_i (mm) | Therm. signal at the spot $\Delta S(r_i, r_0)$ (V) | Therm. signal at the right side of the ring, $S_i^{\text{right}}(L, \infty)$ (V) | Therm. signal at the left side of the ring, $S_i^{\text{left}}(L, \infty)$ (V) | Therm. signal out of the spot, $S_i(L, \infty)$ (V) | σ |
|----------------------------|---|---|---|--|----------|
| 1.5 | -2.989×10^{-5} | – | – | – | 0.0000 |
| 5.0 | -1.271×10^{-5} | 6.443×10^{-2} | 6.166×10^{-2} | 6.304×10^{-2} | 0.0003 |
| 7.5 | 3.263×10^{-6} | 6.513×10^{-2} | 6.079×10^{-2} | 6.296×10^{-2} | 0.0005 |
| 10.0 | 2.545×10^{-5} | 6.666×10^{-2} | 5.957×10^{-2} | 6.311×10^{-2} | 0.0009 |
| 12.5 | 4.204×10^{-5} | 6.707×10^{-2} | 5.897×10^{-2} | 6.302×10^{-2} | 0.0011 |
| 15.0 | 5.238×10^{-5} | 6.834×10^{-2} | 5.861×10^{-2} | 6.347×10^{-2} | 0.0013 |
| 17.5 | 5.376×10^{-5} | 6.986×10^{-2} | 5.843×10^{-2} | 6.414×10^{-2} | 0.0013 |
| 20.0 | 6.294×10^{-5} | 7.097×10^{-2} | 5.875×10^{-2} | 6.486×10^{-2} | 0.0015 |
| 25.0 | 7.467×10^{-5} | 7.089×10^{-2} | 6.013×10^{-2} | 6.551×10^{-2} | 0.0016 |
| 30.0 | 8.069×10^{-5} | 7.291×10^{-2} | 5.944×10^{-2} | 6.617×10^{-2} | 0.0017 |
| 35.0 | 9.254×10^{-5} | 7.106×10^{-2} | 5.753×10^{-2} | 6.429×10^{-2} | 0.0019 |
| 50.0 | 1.205×10^{-4} | 6.546×10^{-2} | 4.873×10^{-2} | 5.709×10^{-2} | 0.0024 |

Table 6 SSE results for VEGA radiation thermometer using successive radiation rings (900 nm)

| Aperture radius r_i (mm) | Therm. signal at the spot $\Delta S(r_i, r_0)$ (V) | Therm. signal at the right side of the ring, $S_i^{\text{right}}(L, \infty)$ (V) | Therm. signal at the left side of the ring, $S_i^{\text{left}}(L, \infty)$ (V) | Therm. signal out of the spot, $S_i(L, \infty)$ (V) | σ |
|----------------------------|---|---|---|--|----------|
| 1.5 | -2.241×10^{-5} | – | – | – | 0.0000 |
| 5.0 | 7.097×10^{-4} | 1.425×10^{-1} | 1.366×10^{-1} | 1.395×10^{-1} | 0.0052 |
| 7.5 | 8.756×10^{-4} | 1.444×10^{-1} | 1.347×10^{-1} | 1.395×10^{-1} | 0.0064 |
| 10.0 | 9.693×10^{-4} | 1.462×10^{-1} | 1.352×10^{-1} | 1.407×10^{-1} | 0.0071 |
| 12.5 | 1.049×10^{-3} | 1.485×10^{-1} | 1.348×10^{-1} | 1.416×10^{-1} | 0.0077 |
| 15.0 | 1.100×10^{-3} | 1.499×10^{-1} | 1.360×10^{-1} | 1.429×10^{-1} | 0.0080 |
| 17.5 | 1.151×10^{-3} | 1.519×10^{-1} | 1.369×10^{-1} | 1.444×10^{-1} | 0.0084 |
| 20.0 | 1.198×10^{-3} | 1.553×10^{-1} | 1.373×10^{-1} | 1.463×10^{-1} | 0.0087 |
| 25.0 | 1.290×10^{-3} | 1.593×10^{-1} | 1.335×10^{-1} | 1.464×10^{-1} | 0.0093 |
| 30.0 | 1.388×10^{-3} | 1.629×10^{-1} | 1.244×10^{-1} | 1.436×10^{-1} | 0.0100 |
| 35.0 | 1.497×10^{-3} | 1.648×10^{-1} | 1.132×10^{-1} | 1.390×10^{-1} | 0.0108 |
| 50.0 | 1.804×10^{-3} | 1.602×10^{-1} | 1.040×10^{-1} | 1.321×10^{-1} | 0.0131 |

component because, especially when large sources are used, it is difficult to have good uniformity over the whole aperture. With the integrating sphere used here, the component from $u(S(L, \infty))$, due to the non-uniformity, is the largest component in Tables 3 and 4, and it becomes more important when the size of source increases.

It is possible to reduce this component by calculating the SSE as a sum of successive contributions of radiating rings (Eq. 10). When Eq. 10 is used, the uncertainty due to the non-uniformity is reduced (see Fig. 3), particularly for large apertures (when the integrating sphere is less uniform). The method shown here can be useful in calculating the SSE uncertainty when non-uniform integrating spheres are used.

Table 7 SSE uncertainty results for IKE LP2 radiation thermometer using successive radiation rings (650 nm)

| Aperture radius r_i (mm) | σ | $\sum_{j=1}^i s'_{2ij}^2 u^2$ ($\Delta S(r_j, r_0)$) | $s_{3i}^2 u^2 (S_b)$ | $\sum_{j=1}^i s'_{1ij}^2 u^2$ ($S_j(L, \infty)$) | $U(\sigma) k = 2$ |
|-------------------------------|----------|---|------------------------|---|-------------------|
| 1.5 | 0.0000 | – | – | – | – |
| 5.0 | 0.0003 | 1.62×10^{-16} | 9.08×10^{-11} | 1.19×10^{-11} | 0.00002 |
| 7.5 | 0.0005 | 1.28×10^{-15} | 9.08×10^{-11} | 3.74×10^{-11} | 0.00002 |
| 10.0 | 0.0009 | 1.83×10^{-15} | 9.08×10^{-11} | 1.67×10^{-10} | 0.00003 |
| 12.5 | 0.0011 | 8.65×10^{-9} | 9.08×10^{-11} | 2.63×10^{-10} | 0.00019 |
| 15.0 | 0.0013 | 8.65×10^{-9} | 9.08×10^{-11} | 3.15×10^{-10} | 0.00019 |
| 17.5 | 0.0013 | 8.65×10^{-9} | 9.08×10^{-11} | 3.16×10^{-10} | 0.00019 |
| 20.0 | 0.0015 | 8.65×10^{-9} | 9.08×10^{-11} | 3.75×10^{-10} | 0.00019 |
| 25.0 | 0.0016 | 8.65×10^{-9} | 9.08×10^{-11} | 4.47×10^{-10} | 0.00019 |
| 30.0 | 0.0017 | 8.65×10^{-9} | 9.08×10^{-11} | 4.76×10^{-10} | 0.00019 |
| 35.0 | 0.0019 | 8.65×10^{-9} | 9.08×10^{-11} | 6.01×10^{-10} | 0.00019 |
| 50.0 | 0.0024 | 8.73×10^{-9} | 9.08×10^{-11} | 2.32×10^{-9} | 0.00021 |

Table 8 SSE uncertainty results for VEGA radiation thermometer using successive radiation rings (900 nm)

| Aperture radius r_i (mm) | σ | $\sum_{j=1}^i s'_{2ij}^2 u^2$ ($\Delta S(r_j, r_0)$) | $s_{3i}^2 u^2 (S_b)$ | $\sum_{j=1}^i s'_{1ij}^2 u^2$ ($S_j(L, \infty)$) | $U(\sigma) k = 2$ |
|-------------------------------|----------|---|------------------------|---|-------------------|
| 1.5 | 0.0000 | – | – | – | – |
| 5.0 | 0.0052 | 0.00×10^0 | 1.04×10^{-10} | 4.10×10^{-9} | 0.00013 |
| 7.5 | 0.0064 | 2.47×10^{-14} | 1.04×10^{-10} | 4.67×10^{-9} | 0.00014 |
| 10.0 | 0.0071 | 3.43×10^{-14} | 1.04×10^{-10} | 4.89×10^{-9} | 0.00014 |
| 12.5 | 0.0077 | 3.23×10^{-9} | 1.04×10^{-10} | 5.14×10^{-9} | 0.00018 |
| 15.0 | 0.0080 | 3.23×10^{-9} | 1.04×10^{-10} | 5.14×10^{-9} | 0.00018 |
| 17.5 | 0.0084 | 3.23×10^{-9} | 1.04×10^{-10} | 5.27×10^{-9} | 0.00019 |
| 20.0 | 0.0087 | 3.23×10^{-9} | 1.04×10^{-10} | 5.43×10^{-9} | 0.00019 |
| 25.0 | 0.0093 | 3.23×10^{-9} | 1.04×10^{-10} | 5.69×10^{-9} | 0.00019 |
| 30.0 | 0.0100 | 3.23×10^{-9} | 1.04×10^{-10} | 8.06×10^{-9} | 0.00021 |
| 35.0 | 0.0108 | 3.23×10^{-9} | 1.04×10^{-10} | 1.34×10^{-8} | 0.00026 |
| 50.0 | 0.0131 | 3.24×10^{-9} | 1.04×10^{-10} | 2.27×10^{-8} | 0.00032 |

References

1. H.W. Yoon, D.W. Allen, R.D. Saunders, Metrologia **42**, 89 (2005)
2. P. Bloembergen, Y. Duan, R. Bosma, Z. Yuan, in *Proceedings of TEMPMEKO '96, 6th International Symposium on Temperature and Thermal Measurements in Industry and Science*, ed. by P. Marcarino (Levrotto and Bella, Torino, 1997), pp. 261–266, ISBN 8882180999
3. G. Machin, R. Sergienko, in *Proceedings of TEMPMEKO 2001, 8th International Symposium on Temperature and Thermal Measurements in Industry and Science*, ed. by B. Fellmuth, J. Seidel, G. Scholz (VDE Verlag, Berlin, 2002), pp. 155–160, ISBN 3800726769
4. P. Saunders, Metrologia **40**, 93 (2003)